Thermodynamics and kinetics of elastic calorific effect in shape memory alloys

© G.A. Malygin

Ioffe Institute,
St. Petersburg, Russia

E-mail: malygin.ga@mail.ioffe.ru

The mechanism of elastic calorific effect in crystals of alloys with SME is theoretically discussed within the framework of the theory of diffuse thermoelastic martensitic transitions, that the structural transitions in alloys with shape memory effect (SME) are. The theory provides an adequate description of the elastic calorific effect under adiabatic unloading of the crystal and stable behavior of the martensitic transition. Flexibility of the theory is also applicable to kinetically unstable (with a burst) martensitic transitions caused by structural features of the crystal, as is the case, according to literature, of $Ni_{50}Fe_{19}Ga_{27}Co_4$ alloy crystal compression along the direction of [011].

Key words: alloys with SME, elastic calorific effect, thermoelastic martensitic transitions, stable and unstable kinetics of martensitic transition.

1. Introduction

Alloys with shape memory effect (SME) are sensitive to magnetic, electrical, and mechanical impacts. Currently these alloys are used as working elements in various devices of micro- and nano-electronics, robotics, medicine, and industry. In the recent decade the attention of researchers is attracted to the effect of adiabatic heating and cooling of crystals of these alloys near the critical temperature of martensitic transition in them. The effect emerges in case of quick switching on (off) of magnetic [1–3] or electric [4] fields, or as a result of mechanical stress applied to or released from a crystal [5–8]. The achieved magnetic calorific, electric calorific, and elastic calorific (EC) effects ΔT_{ad} can be as high as $5-20$ K [1–8]. The adiabatic heating or cooling of the alloy is sourced from isothermal change in its entropy ΔS at the direct and reverse martensitic transition as phase transitions of the first kind. As compared with the adiabatic compression and expansion of steam or gas, the above-mentioned calorific effects in crystals with SME has a technological benefit, especially as related to building up solid state low-volume refrigerator devices.

The research activities conducted at present time have shown that the magnetic calorific effects in ferromagnetic alloys with SME, despite their sufficiently large value at the first change in magnetic field strength, demonstrate lower and unstable values under further changes in the field strength [1–3]. The cause of this instability is related to unstable magnetization of the alloy under adiabatic changes in magnetic field. In addition, the magnetic calorific effect is observed in a relatively narrow temperature range: $(10-20$ K$)$ [1]. The EC-effect is observed in a considerably wider temperature range. For example, in crystals of

$Cu_{68}Zn_{16}Al_{16}$ [6] and $Ni_{50}Fe_{19}Ga_{27}Co_4$ [7,8] alloys it is 150 K (Fig. 1). Experiments with $Ni_{50}Mn_{34.8}In_{15.2}$ alloy [9] on the basis of $4 \cdot 10^3$ adiabatic cycles have shown good cyclic stability of the elastic calorific effect. In [10], it is demonstrated on $Ni_{50.4}Ti_{49.6}$ alloy films with a thickness of $20\,\mu$m that the adiabatic EC-effect is really achieved at strain rates higher than $0.1\,s^{-1}$ and is nearly absent at a strain rate less than $10^{-3}\,s^{-1}$.

One more thing was found recently while investigating the elastic calorific effects in crystals of the $Ni_{50}Fe_{19}Ga_{27}Co_4$ alloy [7,8]. It is the sensitivity of this effect to the crystallographic direction of applying the mechanic compression load to the crystal [7]. Applying the compression stress along the [111] axis of the crystal is not accompanied with a considerable effect of its adiabatic heating or cooling. However, the elastic calorific effect is fully observed, if the crystal is adiabatically loaded and unloaded along the [001] axis of the crystal [7] (Fig. 1). Stress-strain diagrams of crystal compression along the [001] direction have traditional behavior of one-stage curves of pseudoelastic strain. What is unusual is the temperature dependence of the elastic calorific effect in crystals of the $Ni_{50}Fe_{19}Ga_{27}Co_4$ alloy, if the crystal deformed by a compression along the [011] axis is adiabatically unloaded [8] (Fig. 2, triangles). It can be seen that above the temperature of 388 K the effect of adiabatic cooling of the crystal is developed in a way that is qualitatively similar to that in crystals of this alloy under its compression along the [001] axis (Fig. 2, circles). Also, it can be seen that in a considerable temperature range below 388 K the effect of adiabatic cooling is nearly absent in the crystal deformed by compression along the [011] direction. It means that, as shown below in this article (section 4), the temperature of 388 K is critical for the sharp
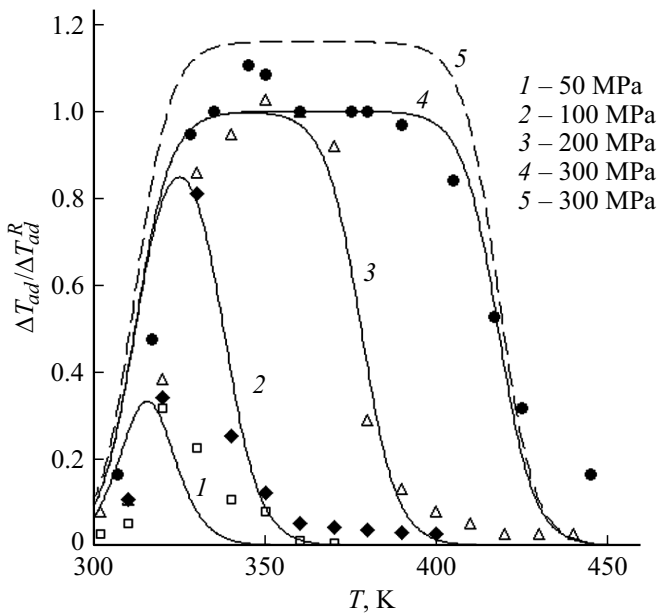
Figure 1. Temperature dependencies of the elastic calorific effect in $\Delta T_{ad}/\Delta T_{ad}^R - T$ coordinates, where $\Delta T_{ad}^R = 9.5$ K, in a crystal of $Ni_{49}Fe_{18}Ga_{27}Co_4$ alloy under its unloading from different stresses in a range of $50-300$ MPa in the stress-strain diagram of crystal compression along the [001] direction. Experimental points — [7], curves *1–4* and dashed line — according to equations $(5)-(6)$.
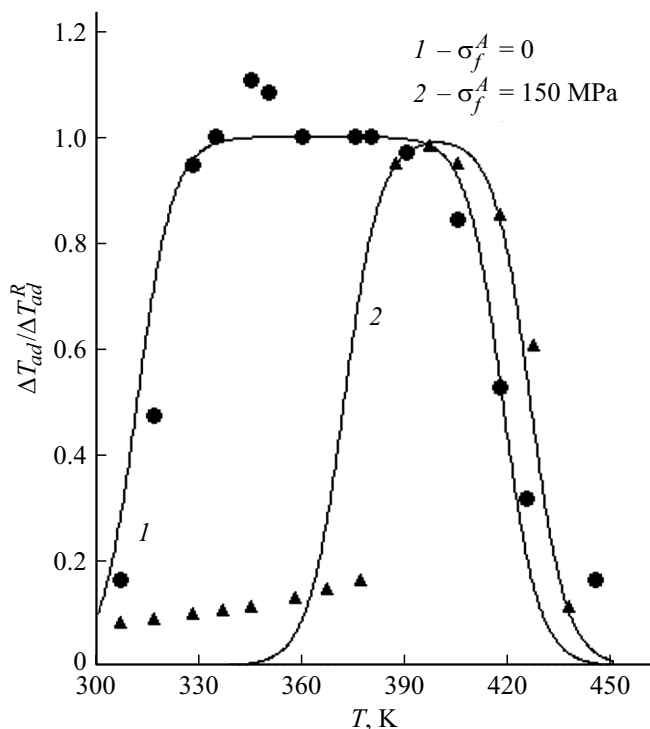
Figure 2. Temperature dependencies of the elastic calorific effect in $\Delta T_{ad}/\Delta T_{ad}^R - T$ coordinates in crystals of $Ni_{49}Fe_{18}Ga_{27}Co_4$ allot under unloading from 300 MPa stress in the stress-strain diagram of crystal compression along [011] ($\Delta T_{ad}^R = 6.1$ K) and [001] ($\Delta T_{ad}^R = 9.5$ K) axes, respectively. Experimental points [8]: circles — along the [001] axis, triangles — along the [011] axis. Curves *1* and *2* — according to equations (5) and (8).

drop of martensite volume fraction in the crystal under its unloading. Another peculiarity of stress-strain diagrams of this alloy crystal compression along the [011] direction is the presence of a sharp stress drop accompanied of intense acoustic emission [8]. Similar stress drops were observed before in two-stage diagrams of $Ni_{49}Fe_{18}Ga_{27}Co_6$ alloy crystal compression along the [011] direction and no such drops were observed under its compression along the [001] axis [11]. According to [11,12], the emergence of abnormal stress drops in this alloy deformed in the [011] direction is related to the emergence of interphase elastic stresses in the crystal with their burst-like martensite relaxation [12]. The interphase stresses are resulted from the change in habit plane orientation in the martensite under crystal compression along the [011] axis as compared with its compression along the [001] axis when there is no such orientation mismatch .

The purpose of this work is to develop thermodynamically and kinetically proved theory of the elastic calorific effect in alloys with SME. It is analyzed and simulated using the theory of diffuse thermoelastic martensitic transitions (DTMT) [13,14], which is based on thermodynamic and kinetic relationships and sensitive to the crystal structure at the meso level. Section 2 includes main relationships of this theory that define isothermal changes in crystal entropy $\Delta S < 0$ and quantity of the elastic calorific effect $\Delta T_{ad} < 0$ under adiabatic unloading of the crystal. In the third section these relationships are used to analyze the elastic calorific effect in crystals oriented under compression in the direction of [001] axis, i.e. at absence of interphase stresses in the crystal, section 4 covers the case of these stresses present in the crystal deformed by compression along the [011] direction. The technical results are compared with experimental results obtained during investigation of the elastic calorific effect in crystals of the $Ni_{50}Fe_{19}Ga_{27}Co_4$ alloy with corresponding orientations [7,8].

2. Elastic calorific effect and theory of DTMT

The isothermal change in entropy of the crystal $\Delta S < 0$ that define the quantity of EC-effect $\Delta T_{ad} < 0$ depends on the set martensitic strain of the crystal ε according to the thermodynamic relationship [5]:

$$\Delta S(\varepsilon) = -\int_0^\varepsilon \left(\frac{\partial \sigma}{\partial T}\right) d\varepsilon, \qquad (1)$$

where T — temperature, σ —mechanical stress applied to the crystal. According to the theory of DMT, the martensitic strain ε changes proportionally to the relative volume of the crystal φ_M occupied by the martensite. With one-stage behavior of the martensitic transition, this volume is defined by kinetic and thermodynamic relationships [14]:

$$\varepsilon = \varepsilon_m \varphi_M, \quad \varphi_M = \frac{1}{1 + \exp(\Delta U/k_B T)}, \qquad (2a)$$

where ε_m — strain of the lattice at its structural reconstruction, $\Delta U = \omega \Delta u$ — change in free energy of the alloy under the emergence of a new phase seed in it with a volume of ω, Δu — bulk density of the phase transition free energy,

$$\Delta u = q \frac{T - T_c}{T_c} - \varepsilon_m \sigma - W_{el}, \qquad (2b)$$

$q = \Delta S T_c$ — heat of transition, ΔS — change in entropy under martensitic transition, $T_c = (M_s + A_f)/2$ — characteristic temperature of the martensitic transformation with absence of external and internal stresses, k_B — Boltzmann constant, $W_{el} = \sigma_e \varepsilon_{el}(\varphi_M)$ — internal elastic energy related to the transition [12]:

$$W_{el}(\varphi_M) = \sigma_e \varepsilon_m \varphi_M (1 - \varphi_M), \qquad (2c)$$

where σ_e — interphase stresses at the martensite and austenite phase interface (lamellae). Equations $(2a)-(2c)$ describe the equilibrium of martensitic φ_M and austenitic $\varphi_A = 1-\varphi_M$ phases in a crystal. The presence of structurally sensitive elementary volume of transformation ω in equation $(2a)$ means that the displacement of martensitic transformation (MT) dislocations over the habit plane is spatially limited. For example, it is limited by the size of homogenous [15] or heterogenous sources of MT dislocations or by the size of cross-section of nano- or microcrystal [16].

By plugging equations $(2b)$ and $(2c)$ into $(2a)$ and solving this equation for stress σ, we get its dependence on temperature, interphase stresses σ_e, and martensitic strain of the crystal $\varepsilon = \varepsilon_m \varphi_M$,

$$\sigma = \sigma_m \left[\frac{T - T_c}{T_c} - a_e \frac{\varepsilon}{\varepsilon_e} \left(1 - \frac{\varepsilon}{\varepsilon_e} \right) + \frac{1}{\bar{\omega}} \ln \left(\frac{\varepsilon/\varepsilon_m}{1 - \varepsilon/\varepsilon_m} \right) \right], \qquad (3)$$

where $\sigma_m = q/\varepsilon_m = (d\sigma/dT)_K T_c$, $(d\sigma/dT)_K$ — Clapeyron–Clausius coefficient, $a_e = \sigma_e/\sigma_m$, $\bar{\omega} \approx \omega q/k_B T_c$. By partially differentiating (3) with respect to T, we get $(\partial \sigma/\partial T)_e = (d\sigma/dT)_K$ and hence the change in crystal entropy according to thermodynamic relationship (1) is

$$\Delta S(\varepsilon) = -\left(\frac{d\sigma}{dT} \right)_K (\varepsilon - \varepsilon_0)$$

$$= -\varepsilon_m \left(\frac{d\sigma}{dT} \right)_K [\varphi_M(T, \sigma, \sigma_e) - \varphi_0]. \qquad (4a)$$

It is defined by the martensitic strain ε that depends on martensite concentration in the crystal $(2a)$. The condition of $\Delta S(\varepsilon_0) = 0$ defines the integrating constant of equation (1)

$$\varepsilon_0(T, \sigma_e) = -\varepsilon_m \left(\frac{d\sigma}{dT} \right)_K [-\varphi_0]$$

$$= -\varepsilon_m \left(\frac{d\sigma}{dT} \right)_K [-\varphi_M(T, 0, \sigma_e)]. \qquad (4b)$$

As a result, we get the following relationship for the quantity of the elastic calorific effect (decrease in crystal temperature under its adiabatic unloading):

$$\Delta T_{ad} = \frac{T_c}{C_p} \Delta S = -\varepsilon_m \left(\frac{d\sigma}{dT} \right)_K \frac{T_c}{C_p} \Delta \varphi_M(T, \sigma, \sigma_e)$$

$$= -\frac{q}{C_p} \Delta \varphi_M(T, \sigma, \sigma_e), \qquad (5a)$$

$$\Delta \varphi_M(T, \sigma, \sigma_e) = \varphi_M(T, \sigma, \sigma_e) - \varphi_M(T, \sigma = 0, \sigma_e), \quad (5b)$$

where C_p — heat capacity of the crystal, ΔS and q — change in entropy and heat of the reverse martensitic transition, respectively $\Delta \varphi_M(T, \sigma, \sigma_e)$ — volume fraction of martensite, that defines the quantity of elastic calorific effect as a function of temperature T, stress σ applied to the crystal, and presence of internal elastic stresses σ_e in it.

3. Elastic calorific effect under absence of interphase stresses

Figure 3 illustrates temperature dependencies of martensite volume fractions $\varphi 1_M(T, 0, \sigma)$ (curve *1*) and $\varphi 2_M$ (curve *2*) according to equations (2), as well as their difference $\Delta \varphi_M = \varphi 2_M - \varphi 1_M$ (curve *3*) under absence of
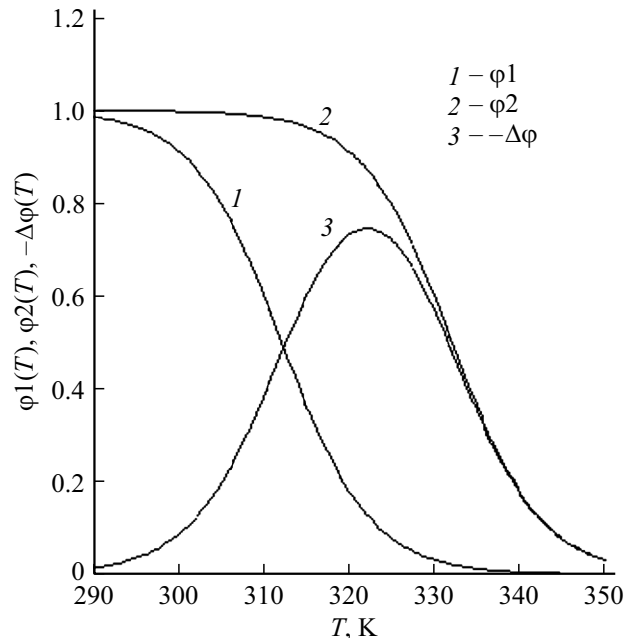
Figure 3. The temperature dependencies according to equations (5b) and (6) for volume fractions of martensite φ without (curve *1*) and with stress $20\,\text{MPa}$ (curve *2*) applied to the crystal, as well as the difference between these fractions (curve *3*), that defines the change in entropy ΔS^R and temperature of the crystal ΔT_{ad} at its unloading from the aforementioned stress.

internal elastic stresses in the crystal ($\sigma_e = 0$), where

$$\varphi 1_M(T, 0, 0) = \left[1 + \exp\left(\bar{\omega} \left(\frac{T - T_c}{T_c} \right) \right) \right]^{-1},$$

$$\varphi 2_M(T, \sigma, 0) = \left[1 + \exp\left(\bar{\omega} \left(\frac{T - T_c}{T_c} - \frac{\sigma - \Delta\sigma_h}{\sigma_m} \right) \right) \right]^{-1},$$

(6)

$\Delta\sigma_h = (d\sigma/dT)_K \Delta T_h$ — hysteresis of stresses at the direct and reverse martensitic transformation, $\Delta T_h = (A_s + A_f - M_s - M_f)/2$ — equivalent $\Delta\sigma_h$ temperature hysteresis. When estimating in (6) the values of parameters $T_c = 312$ K, $\sigma_m = 780$ MPa, $\bar{\omega} = 60$, $\Delta T_h = 14.6$ K and $\Delta\sigma_h = 35$ MPa, the notation of (3) and data of [7] for crystals of NiFeGaCo alloy were used: $M_s = 304$ K, $M_f = 296$ K, $A_s = 310$ K, $A_f = 320$ K, $(d\sigma/dT)_K = 2.5$ MPa/K. In Fig. 3 curve *1* shows temperature dependence of concentration φ of thermal elastic martensite in the crystal, and curve *2* shows growth of this concentration as a result of stress $\sigma = 20$ MPa applied to the crystal. Curve *3* demonstrates temperature dependence of the martensite volume fraction $\Delta\varphi_M$, which, according to equation (5), defines the isothermal change in entropy ΔS and the quantity of elastic calorific effect at crystal unloading down to $\sigma = 0$. It can be seen, that the martensite volume fraction $\Delta\varphi$ first increases with increase in temperature due to the strain martensite. Then it achieves its maximum and decreases down to zero due to transition of the strain martensite to austenite under the impact of high temperature.

This bell-shaped behavior is exactly the behavior of temperature dependencies of elastic calorific effect ΔT_{ad} in crystals of the Ni$_{49}$Fe$_{18}$Ga$_{27}$Co$_4$ alloy (Fig. 1) under their unloading from different stresses on the diagram of crystal compression (curves *1–4*). In Fig. 1, these dependencies are represented in reduced coordinates $\Delta T_{ad}/\Delta T_{ad}^R - T$ according to equations (5) and values of the parameters specified in (6), where $\Delta T_{ad}^R = q/C_p$. According to calorimetric data [7] ($q = 280$ J/mol, $C_p = 26$ J/mol $\cdot$ K), maximum adiabatic decrease in temperature ΔT_{ad}^R should be ≈ 11 K (Fig. 1, dashed line). However, the experiment shows a lower value: $\Delta T_{ad}^R \approx 9.5$ K. Discussing this mismatch, authors of [7] have made a guess that it may be caused by adiabatic nature of the alloy crystal unloading procedure (0.3 s^{-1}). Also worth noting are the results obtained in [8] for the diffraction analysis of structures of thermal elastic martensite and strain martensite in the alloy under research. It is found that in the first case it is 14M modulated martensite, and in the second case it is non-modulated tetragonal L1$_0$ martensite. It means that at temperatures before the maximum of curves *1−4* (Fig. 1) L2$_1$ austenite transforms into L1$_0$ martensite in two stages L2$_1 \rightarrow$ 14M $\rightarrow$ L1$_0$.

One final comment on this section is that the $\bar{\omega} = 60$ parameter in relationships (6) corresponds (at $q = 280$ J/mol, $T_c = 312$ K and mol $= 7.84$ cm^3) to the elementary volume of martensite $\omega = \bar{\omega}(k_B T_c/q) = 6.6$ nm^3. If a homogenous source forms one MT dislocation loop with a diameter

of d, the elementary volume of the phase transformation is $\omega = (\pi d^2/4) a_0$, where $a_0 = 0.4$ nm [7] is the distance between adjacent habit planes in the martensite. The above estimate of elementary volume of the transformation has a correspondent diameter of dislocation loop of the martensite transformation $d = (4\omega/\pi a_0) \approx 4.6$ nm, which is close the the size of the homogenous source of MT dislocations [15].

4. Impact of interphase stresses on the elastic calorific effect

As previously stated, in the case of Ni$_{49}$Fe$_{18}$Ga$_{27}$Co$_4$ alloy crystals compression along the [011] axis, compression diagrams contain an elongated interval of strain where stress drop is observed, which is an indication of unstable (burst-like [11,12]) behavior of the martensitic transition in this alloy [8]. To make clear this thing, Fig. 4, *a* and *b* shows results of compression diagrams simulation for crystals of
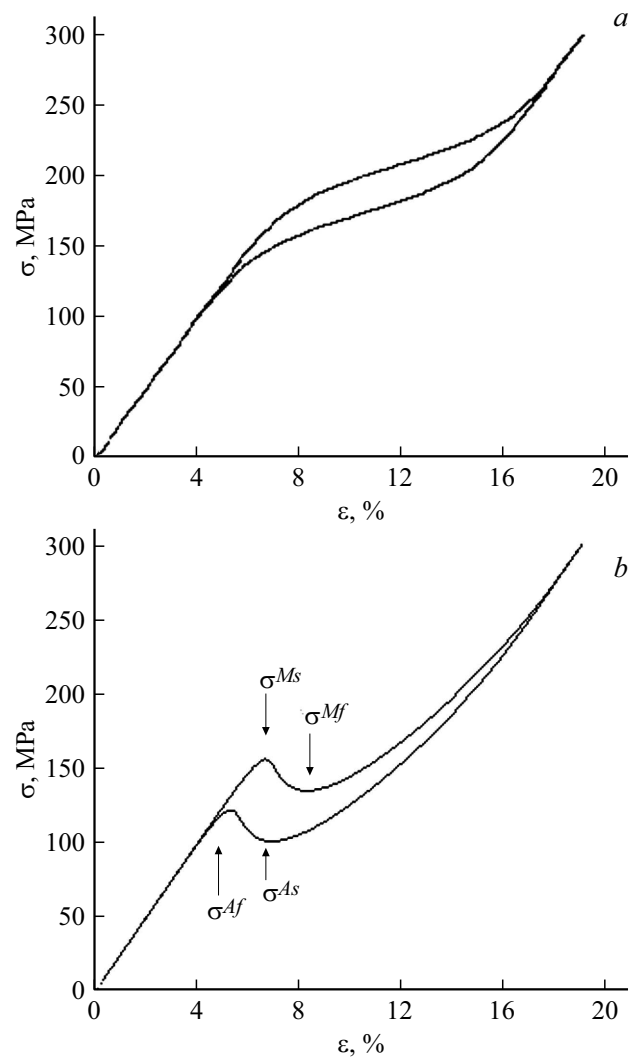
Figure 4. Crystal compression diagrams of the NiFeGaCo alloy without (*a*) and with (*b*) interphase stresses in the crystals according to equation (7) (see detail in the text).

this alloy within the framework of DTMT theory without interphase stresses in the crystal ($\sigma_e = 0$) (Fig. 4, a) and with interphase stresses ($\sigma_e \neq 0$) (Fig. 4, b), respectively. Taking into account the elastic strain of the crystal under compression $\varepsilon_E(\sigma) = \sigma/E$, the equation to calculate dependence of the stress σ on the sum compression strain $\varepsilon = \varepsilon_E + \varepsilon_M$ has the following form

$$\varepsilon = \varepsilon_E + \varepsilon_m \left[1 + \exp\left(\bar{\omega}\left(\frac{T - T_c}{T_c} - \frac{\sigma_e}{\sigma_m}(\varepsilon - \varepsilon_E) \right. \right. \right.$$

$$\left. \left. \left. \times \left(1 - (\varepsilon - \varepsilon_E) \right) - \frac{\sigma \mp \Delta\sigma_h}{\sigma_m} \right) \right) \right]^{-1}, \qquad (7)$$

where $\varepsilon_M = \varepsilon_m \varphi_M$ is martensitic strain (2a), $E = (E_M + E_A)/2$ — mean modulus of elasticity, σ_h — stress hysteresis under loading ($-$) and unloading ($+$) of the crystal by the compression stress. The $\sigma(\varepsilon)$ dependence is implicitly contained in equation (7), therefore the equation was solved numerically with the following values of variables and parameters: $T = 388\,\mathrm{K}$, $\varepsilon_m = 7\%$, $E = 2.5\,\mathrm{GPa}$, without interphase stresses ($\sigma_e = 0$, $\sigma_h = 17\,\mathrm{MPa}$) and with interphase stresses ($\sigma_e = 280\,\mathrm{MPa}$, $\sigma_h = 17\,\mathrm{MPa}$); other parameters had the same values as were previously used to build the curves in Fig. 1. As can be seen from comparison of curves in Fig. 4, a and b, the existence of interphase stresses in the crystal promotes the unstable behavior of martensitic transition. As a result, instead of plateau (Fig. 4, a) an interval of deforming stress drop emerges in the compression diagram. In the real diagram of the $Ni_{50}Fe_{19}Ga_{27}Co_4$ crystal compression in the direction of [011] axis, as well as in the case of $Ni_{49}Fe_{18}Ga_{27}Co_6$ alloy crystals [12], this drop is composed of two stages: at the first stage twinned $L1_0$ martensite (14M) is formed, and at the second stage the 14M martensite is detwinned. Fig. 4, b illustrates only one of these stages (in [12] both these stages are simulated within the framework of DTMT theory). Results of the simulation [12] in line with experiments have shown that with increase in temperature the two-stage drop of stress in compression diagrams of $Ni_{49}Fe_{18}Ga_{27}Co_6$ alloy crystals changes to one-stage drop, i.e. the $L2_1$ austenite transforms directly into the tetragonal $L1_0$ martensite, which also takes place in the case of $Ni_{50}Fe_{19}Ga_{27}Co_4$ alloy crystals [8].

In Fig. 4, b σ^{Ms} and σ^{Mf} stresses in the compression diagram mark the start and the end of the direct martensitic transformation, while σ^{As} and σ^{Af} mark the reverse martensitic transformation in the crystal. At a stress of σ^{Af}, martensite in the crystal is completely transformed to austenite. Hence the volume fraction of martensite $\Delta\varphi_M$ that defines the isothermal change in entropy ΔS and the elastic calorific effect ΔT_{ad}, is equal to:

$$\Delta\varphi_M(T, \sigma, \sigma_e) = \varphi_M 2(T, \sigma, \sigma_e) - \varphi_M 1(T, \sigma^{Af}, \sigma_e), \quad (8a)$$

where

$$\varphi1_M = \left[1 + \exp\left(\bar{\omega}\left(\frac{T - T_c}{T_c} - \frac{\sigma^{Af} + \sigma_h}{\sigma_m} \right) \right) \right]^{-1},$$

$$\varphi2_M = \left[1 + \exp\left(\bar{\omega}\left(\frac{T - T_c}{T_c} - \frac{\sigma + \sigma_h}{\sigma_m} \right) \right) \right]^{-1}. \quad (8b)$$

In Fig. 2, curve 2 demonstrates the $\Delta T_{ad}(T) \sim \Delta\varphi(T)$ dependence according to equations (8) in $\Delta T_{ad}/\Delta T_{ad}^R - T$ coordinates, where $\Delta T_{ad}^R = 6.1\,\mathrm{K}$. It can be seen that at a temperature of $\approx 388\,\mathrm{K}$ this fraction starts decreasing dramatically and becomes zero. Also, it can be seen that there is a good agreement between theory and experiment. The existence of non-zero values of $\Delta T_{ad} \approx 1\,\mathrm{K}$ below the temperature of $388\,\mathrm{K}$ is related to the hysteresis loss [8]. The dramatic drop of the elastic calorific effect at temperatures below $388\,\mathrm{K}$ is caused by the fact that with interphase stresses the concentration of martensite in the crystal becomes zero at $\sigma^{Af} = 150\,\mathrm{MPa}$ [8], and not at $\sigma^{Af} = 0$ as is the case without these stresses. As a result the elastic calorific effect decreases by

$$\Delta T_{ad}^{Af} = -\Delta T_{ad}^R \left[\varphi_M(T, \sigma^{Af}) - \varphi_M(T, 0) \right]. \quad (8c)$$

The maximum value of elastic calorific effect is $6.1\,\mathrm{K}$ in the temperature range above $388\,\mathrm{K}$, i.e. in the temperature range of stable martensitic transition, which is 36% less than at the crystal compression in the [001] direction.

This decrease becomes even bigger and is equal to 44% when comparing the effect value of $6.1\,\mathrm{K}$ with the theoretical estimate $\Delta T_{ad}^R = 11\,\mathrm{K}$. As $\Delta T_{ad}^R \sim q$, there is a
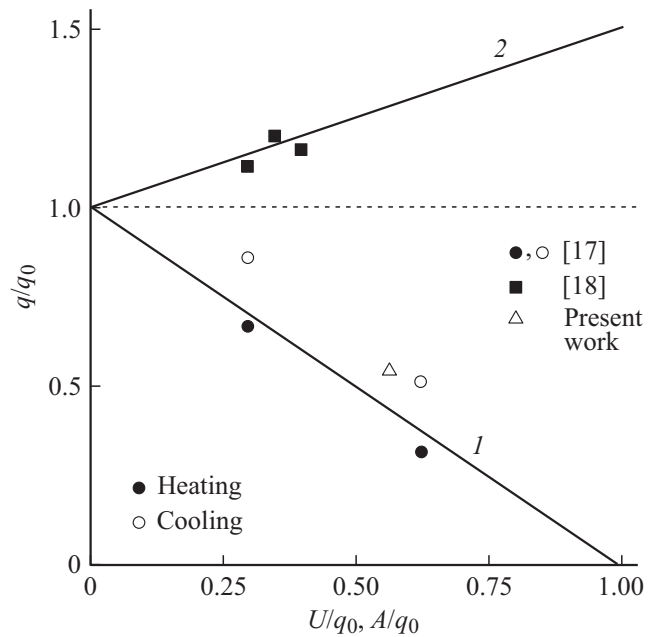
Figure 5. The dependence of martensitic transition heat $q(\sigma_{in})$ in a crystal of Cu−Al−Ni alloy on the energy of internal elastic stresses σ_{in} (curve 1) [17] and on the work $A(\sigma_{ex})$ under the action of externally applied stress σ_{ex} on the crystal (curve 2) [18].

reason to consider that the above-mentioned decrease is related to the decrease in martensitic transition heat q. There is calorimetric data in the literature (Fig. 5, curve *1*) for crystals of the Cu−Al−Ni alloy [17] showing that the heat of martensitic transition depends on the energy $U = \sigma_{in}\varepsilon_{in}$ of internal elastic stresses σ_{in} according to the following law: $q = q_0(1 - U/q_0)$, where q_0 is the heat of transition without internal stresses, ε_{in} — correspondent elastic strains. On the contrary, the heat of transition increases, $q = q_0(1 + A/q_0)$, where $A = \sigma_{ext}\varepsilon_m$ (Fig. 5, curve *2*), if the alloy crystal is under a constant stress (free-hanging weight). It is evident that in the first case in an isolated thermodynamic system a part of heat q_0 is spent for relaxation of internal elastic stresses, in the second case heat q_0 increases due to the work A when the weight is lowered. In our case $q_0 = 280$ J/mol, $\sigma_{in} = \sigma_e = 280$ MPa, $\varepsilon_{in} = \varepsilon_m = 7 \cdot 10^{-2}$, $U(\sigma_{in}) = 153.7$ J/mol and, as a consequence, $U(\sigma_{in})/q_0 = 0.55$, $q(\sigma_{in})/q_0 = 6.1/11 = 0.56$. In Fig. 5, Δ shows the relationship between the heat $q(\sigma_{in})$ and the energy of internal elastic stresses $U(\sigma_{in})$ in a crystal of the $Ni_{50}Fe_{19}Ga_{27}Co_4$ alloy [8]. It can be seen that the relationship is close to curve *1* describing this relationship in crystals of the Cu−Al−Ni alloy [17].

5. Conclusion

Thus, within the framework of thermodynamically and kinetically proved theory of phase transition of the first kind (DTMT theory), which is the case of structural martensite transitions in alloys with shape memory effect, the elastic calorific effect in crystals of alloy with SME is theoretically analyzed. Flexibility and adequacy of the theory is demonstrated not only on kinetically stable martensitic transitions, but also applicable to kinetically unstable (with a burst) martensitic transitions caused by structural features of the crystal, as is the case of compression of $Ni_{50}Fe_{19}Ga_{27}Co_4$ alloy crystals [8] along the [011] direction.

Conflict of interest

The author declares that he has no conflict of interest.

References

[1] K.A. Gschneidner, V.K. Pecharsky, A.O. Tsokol. Rep. Prog. Phys. **68**, 1479 (2005).

[2] A. Planes, L. Mañosa, M. Aset. J. Phys.: Condens. Matter **21**, 233201 (2009).

[3] T. Brück. J. Phys. D **38**, R381 (2005).

[4] A.S. Mishenko, Q. Zhang, J.F. Scott, R.W. Wathmore, N.D. Mathur. Science **311**, issue 5765, 1270 (2006).

[5] E. Bonnot, R. Romero, L. Mañosa, E. Vives, A. Planes. Phys. Rev. Lett. **100**, 125901 (2008).

[6] L. Mañosa, S. Jarque-Farnos, E. Vives, A. Planes. Appl. Phys. Lett. **103**, 211904 (2013).

[7] F. Xiao, M. Jin, J. Liu, X. Jin. Acta Mater. **96**, 292 (2015).

[8] D. Zhao, F. Xiao, Zh. Nie, D. Cong, W. Sun, J. Liu. Scripta Mater. **149**, 6 (2018).

[9] X-M. Huang, L-D. Wang, H-X. Liu, H-L. Yan, N. Jia, B. Yang, Z-B. Li, Yu-D. Zhang, C. Esling, X. Zhao, L. Zuo. Intermetallics **113**, 106579 (2019).

[10] H. Ossmer, F. Lambrecht, M. Gültig, C. Chluba, E. Quandt, V. Kohl. Acta Mater. **81**, 9 (2014).

[11] V.I. Nikolaev, P.N. Yakushev, G.A. Malygin, S.A. Pul'nev, Letters to the Journal of Technical Physics **36**, *19*, 83 (2010) (in Russian).

[12] G.A. Malygin, V.I. Nikolaev, V.M. Krymov, S.A. Pul'nev, S.I. Stepanov, Journal of Technical Physics **89**, 873 (2019) (in Russian).

[13] G.A. Malygin, Physics of the Solid State **36**, 1489 (1994) (in Russian).

[14] G.A. Malygin, Advances in Physical Sciences **171**, 187 (2001) (in Russian).

[15] G.A. Malygin, Physics of the Solid State **63**, 272 (2021) (in Russian).

[16] G.A. Malygin, Physics of the Solid State **61**, 288 (2019) (in Russian).

[17] V.I. Nikolaev, G.A. Malygin, S.A. Pulnev, P.N. Yakushev, V.M. Egorov. Mater. Sci. Forum **738/739**, 51 (2013).

[18] J. Ortin, L. Manosa, C.M. Friend, A. Planes, M. Yoshikawa. Phil. Mag. A **65**, 461 (1992).